

Geostatistical Detection of Thermodynamic Anisotropy in an Atmospheric Boundary Layer Using Small Unmanned Aircraft Systems

Benjamin L. Hemingway
Department of Geography
Oklahoma State University
Stillwater, OK 74078 USA
ben.hemingway@okstate.edu

Amy E. Frazier
Department of Geography
Oklahoma State University
Stillwater, OK 74078 USA
amy.e.frazier@okstate.edu

Abstract

The lowest portion of the Earth's atmosphere, known as the Atmospheric Boundary Layer (ABL), is a critical region of energy exchange and weather development, but it is also one of the most challenging portions of the atmosphere to measure. Current measurement methodologies are either ill-suited or inadequate for collecting meteorological data, such as temperature, that would help us understand the ABL. However, small unmanned aircraft systems (sUAS) have emerged as a dynamic alternative that can fill the spatio-temporal gaps left by traditional atmospheric sensing methods. While the use of sUAS for atmospheric research has accelerated over the last several years, little research has been conducted to characterize the spatial distribution of meteorological variables. The objective of this study is to apply variogram analysis, a common geostatistical technique, to temperature data collected in the ABL to determine the spatial distribution of those values via the maximum and minimum axes of anisotropy and also determine how those measurements compare to mean wind direction measured from a nearby meteorological ground station. Our results show that spatial continuity is greater in directions transverse of the wind, while horizontal mechanical mixing of the ABL in directions analogous to the mean wind direction result in less spatial continuity. These results can aid in future atmospheric mission planning and better understanding of the processes affecting scalar variables, such as temperature in the ABL. Future work is needed to apply these methods in a variety of atmospheric and topographic conditions.

Keywords: drones, unmanned aerial vehicles (UAV), spatial sampling, weather, micrometeorology

1 Introduction

The lowest portion of the Earth's atmosphere, known as the boundary layer (ABL), is a critical region of energy exchange and weather development (Stull, 1988). However, it is also one of the most challenging portions to measure (Frew et al., 2012). Approximately 1-km thick, the ABL is difficult to monitor via manned aircraft, which cannot safely sustain flight at such low altitudes. Weather balloons and radiosondes are an alternative option, but they cannot be controlled from the ground and are not recoverable (Hill et al., 1970).

Networks of ground weather stations (mesonets) capture meteorological measurements near the surface, but towers are usually spaced 10-40 km apart and only extend 10 m above ground (McPherson et al., 2007), which does not fully capture the ABL. Furthermore, the spatial resolution of measurements collected from these towers does not permit observation of microscale surface-atmosphere interactions characterizing the ABL.

Such limitations have spurred advances in atmospheric remote sensing technologies. Satellite-based systems, such as

the Geostationary Operational Environmental Satellite (GOES), have been key for weather forecasting and research over the past several decades; however, satellite-based systems are also limited in their spatial and temporal resolution and the variables they measure. Weather surveillance radar (WSR), in use since the 1950s, has been transformative in forecasting and storm tracking, particularly the WSR-88D radar network (NEXRAD). However, it too is limited in the type of data it can capture (i.e. it cannot measure thermodynamic variables such as temperature) and is limited in the extent of the ABL it can sense due to the angle of the reception cone, Earth's curvature, and interference from mountains and buildings (LaDue et al., 2010; Bendix et al., 2016).

Limitations in ABL sensing technologies have led to the development of small unmanned aircraft systems (sUAS) to fill monitoring gaps (Frew et al., 2012; Frazier et al., 2017; Hemingway et al., 2017). Employing sUAS for atmospheric research dates back to at least 1970 when Hill et al. (1970) captured temperature, pressure, and humidity measurements in the ABL. More recently, sUAS have been used to capture

basic boundary layer measurements (Knuth et al., 2013; Hemingway et al., 2017), sample severe storms (Frew et al., 2012), and monitor air mass boundaries (Houston et al., 2012).

Despite a surge in studies using sUAS for meteorology and atmospheric physics and initial work to determine the vertical distribution of atmospheric parameters (Hemingway et al., 2017), little work has focused on the horizontal distribution of thermodynamic variables, and appropriate sampling scales for these measurements remain unknown. This type of information could ultimately contribute to a better understanding of turbulence by allowing fine-scale characterization of horizontal atmospheric processes.

The objective of this study is to characterize the horizontal (x,y) distribution of temperature using variogram analysis—a common geostatistical technique used in the geographical sciences—of atmospheric samples collected from a sUAS. Specifically, we (1) determine the maximum and minimum directions of spatial continuity (i.e. anisotropy) of temperature and (2) determine how these directions relate to the mean wind direction. This information will aid future mission planning by providing insight into how atmospheric variables are distributed across space and foster a better understanding of the processes taking place in the ABL.

2 Study Site and Data Capture

Data were collected on 16 November 2017 at Gloss Mountain State Park in northwest Oklahoma, USA (36.366°N 98.5788°W). The site is located in a semi-arid grassland ecoregion, and a prominent mesa rises approximately 70 m above the surrounding elevation of 426 m MSL. Conditions were clear with minimal cloud cover at the time of the flights.

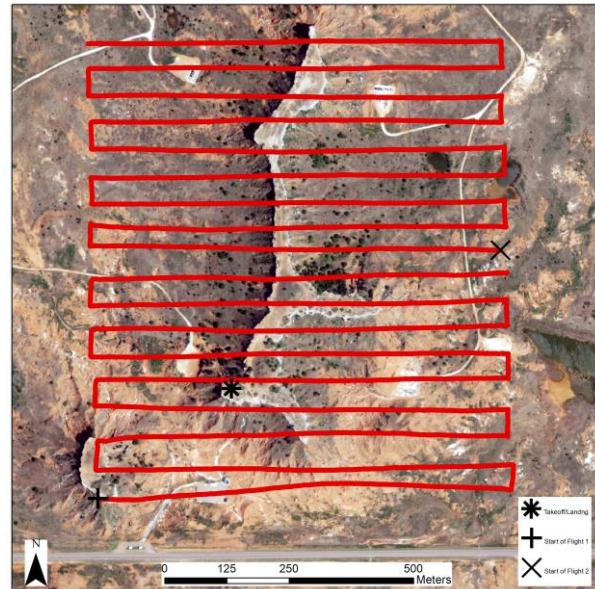
Data were collected using a DJI Phantom 3 (DJI, Shenzhen, China), which is a quad-rotor weighing 1,280 g and measuring 350 mm diagonally in size. The on-board battery provides approximately 25 minutes of flight time, necessitating two segments to survey the entire study area. We captured atmospheric measurements with an iMet XQ sensor (International Met Systems, Grand Rapids, MI, USA). The XQ sensor is a self-contained unit with temperature, relative humidity (RH), and pressure sensors, and a GPS receiver. It weighs 15 g, has a 16-mb storage capacity, and a 120-minute battery life. The temperature sensor is the bead thermistor type with a response time of 2 s and a sampling rate of 1hz.

Surface weather observations during the flights were acquired from the Oklahoma Mesonet—a network of 121 automated meteorological and environmental monitoring stations positioned across the state of Oklahoma, USA (McPherson et al., 2007). The closest station, Fairview, is located 13 km southeast of the study area at an elevation of 405 m. The mean temperature captured at Fairview during the flight was 15.26° C (standard deviation 0.36° C). Mean wind speed was 5.36 m/s (standard deviation 0.62 m/s).

Aircraft take-off and landing occurred on the mesa summit. Eighteen transects, oriented in east-west, were flown (Figure 1). Transects were approximately 830 m and separated by approximately 55 m. Between battery changes, the aircraft was landed, re-launched, and repositioned in the transect formation where data collection was aborted to continue the mission. The approximate flight speed was 8.5 m/s. A

sampling rate of 1 hz resulted in measurements captured approximately every 8.5 m. Data collected during take-off, landings, and re-positioning were excluded, resulting in 1,924 measurements collected between 12:01 and 12:38 Central Standard Time (UTC-6). The average flight altitude was 570.4 m MSL.

Figure 1: Flight path with locations of take-off and landing



3 Data Analysis

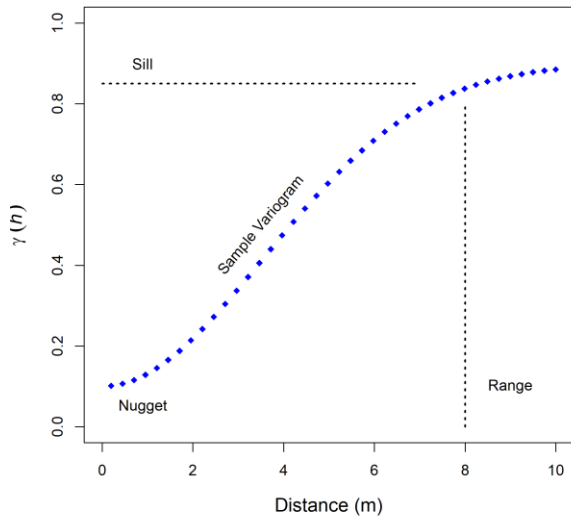
Since the physical processes affecting the spatial variation of geographic phenomena on Earth are complex, their behavior may appear random (Oliver and Webster, 2015). The same is true of atmospheric variables, such as temperature, since movements are governed by the non-linear effects of turbulent motions, or eddies, in the ABL (Stull, 1988). There remains though an inherent structure to the data, and values have a statistical relationship relative to their spatial location. This statistical relationship can be exploited to deconstruct the spatial structure of the variables. The variation between the variable and itself at any two locations is assumed to be a function of space, and this relationship can be described using the variogram, which is a model of the spatial continuity of the data. The estimator for calculating a variogram from sample data is:

$$\hat{\gamma}(h) = \frac{1}{2n(h)} \sum_{i=1}^{n(h)} \{z(x_i) - z(x_i + h)\}^2 \quad (1)$$

where $z(x_i)$ is the observed value of z at location x_i separated by distance h , and n is the number of sample pairs (Cressie, 1993). The variogram has several key characteristics that can be used to describe the spatial structure of the variable (Figure 2). The point at which the semivariance reaches its upper bound and levels off is called the sill. The separation distance between points, or lag distance, at which this occurs is called the range. Beyond the range, spatial dependence decreases. If

the variogram intersects the y-axis at a semivariance value greater than zero, this is called the nugget effect and results from microscale variability at short lag distances or measurement error (Cressie, 1993).

Figure 2: Typical structure and key components of a sample variogram.



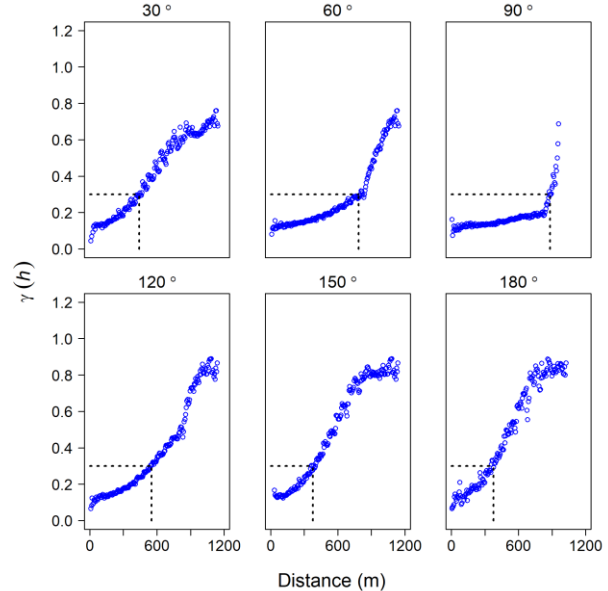
Variogram analysis was completed using the gstat package (Pebesma, 2004) for R. Pairs of points separated by lag distance (h) were grouped into discrete, 6 m-wide bins to allow estimation of the semivariance function at discrete lags. The bin width was slightly less than the spacing between transects following Isaaks and Srivastava (1989). Bins containing fewer than 100 pairs were omitted from analysis so as not to influence variogram behavior with unreliable data. We anticipate the variogram will reach its sill at a distance complementary to the boundary layer thickness, or approximately 1 km (Stull, 1988).

When the statistical relationship between a measured variable is also a function of the direction in which the points are situated, the spatial relationship can be modeled using directional variograms to reveal anisotropy. The angular tolerance for each direction tested should be wide enough that sufficient point pairs are included but narrow enough that the degree of anisotropy is not clouded by combining pairs from too many directions (Isaaks and Srivastava, 1989). Sample variograms were calculated in six directions with a 30° tolerance angle. Directions began at 30° and increased in 30° increments until 180°. Degrees correspond to traditional compass headings where 0° (or 360°) is North, 90° is East, 180° is South, and 270° is West. Since $\gamma(h) = \gamma(-h)$, a sample variogram calculated for any particular direction is the same as it would be calculated in the opposite direction (Isaaks and Srivastava, 1989). For example, the variogram for 180° is identical to that for 360°.

4 Results and Discussion

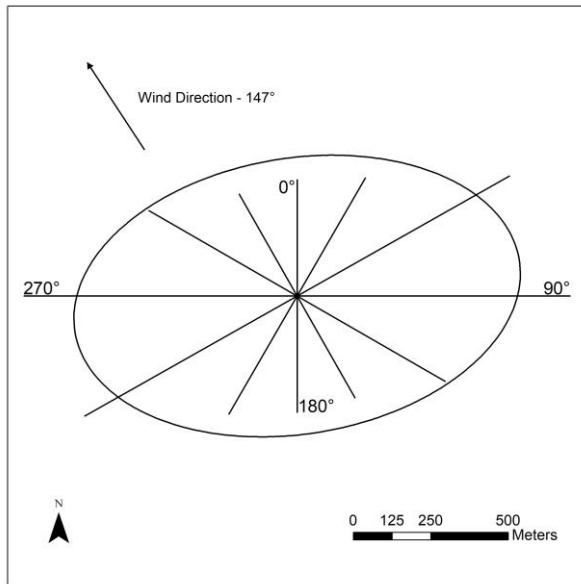
Sample variograms for the six compass directions (Figure 3) show the differences in distance values where $\gamma(h) = 0.3$. A $\gamma(h)$ value of 0.3 was selected for comparison because that value was reached in all six directions at distances with sufficient point pairs to be considered reliable, which is a precondition for determining anisotropy (Isaaks and Srivastava, 1989). In general, this $\gamma(h)$ value is reached at distances increasing from 400 m at 30°, to a maximum value of 900 m for the 90° direction. Distances corresponding to a $\gamma(h)$ value of 0.3 then decrease back down to just under 400 m for the 150° and 180° directions. Long distance values corresponding to $\gamma(h) = 0.3$, such as those observed in the 90° direction, indicate that point pairs separated by a longer distance are more similar, or spatially continuous, than those observed for directions with shorter corresponding distances. By interpreting the distance values corresponding to $\gamma(h) = 0.3$ across all six directions, we can conclude that temperature exhibited strong and coherent spatial continuity in the east-west direction and less continuity in the north-south direction.

Figure 3: Sample variograms calculated for the six directions. Dashed lines indicate distance where $\gamma(h) = 0.3$



To further visualize the anisotropy of the temperature measurements, the distance values for $\gamma(h) = 0.3$ were plotted as lines on a compass rose diagram (Figure 4). Line length corresponds to the distance at which $\gamma(h) = 0.3$ was reached in each directional variogram (Figure 3). Lines are oriented in the direction the sample variogram was calculated. The ellipse (Figure 4) represents two standard deviations of the spatial distribution of the plotted lines. The major axis of the ellipse was computed as 81°, which is the direction where there was the most similarity in temperature values across space (i.e., the most spatial continuity).

Figure 4: Compass rose depicting sample distances corresponding with $\gamma(h) = 0.3$ across the directional sample variograms.



To interpret these findings in the context of the atmospheric conditions during sampling, we acquired wind speed and direction data from the Fairview Mesonet. Mean wind direction during the flight was 147° (SSE to NNW), which corresponds roughly to the 150° directional variogram. This variogram exhibits a classical variogram shape, with semivariance values increasing until a sill is reached at a distance of approximately 800 m (Figure 3). This range distance corresponds approximately to the ABL thickness of about 1 km (Stull, 1988), which met our expectation. The 150° directional variogram was also among the shortest distances at which $\gamma(h) = 0.3$ was reached. Together with the findings above that temperature exhibited strong and coherent spatial continuity in the east-west direction, we can conclude that greater spatial continuity occurs in the direction transverse of the wind. While these findings are not unexpected because there is greater forced convection, or mechanical mixing, in the direction of the wind causing temperature values to be more heterogeneous across space, this hypothesis was not previously verifiable using available sensors and instrumentation.

While these results are encouraging for capturing atmospheric structure, several limitations should be noted. First, we only analyzed data from a single date and location, and repeated analyses under different environmental conditions along with concurrent measurements from multiple sUAS would help improve our understanding of the universality of the findings. While the flight time was minimized, it is possible that the temporal change in temperature across the study area during data collection could have impacted results. Again, having multiple sUAS collecting concurrent measurements could help alleviate this concern in future campaigns. Similarly, the effect of the wind on the sUAS may have contributed to measurement errors.

Wind effects were mitigated by positional stabilization using GPS on the aircraft's autopilot system, but the presence of a nugget on the variograms may be a reflection of measurement error. Additionally, while we did not specifically test for topographic effects, it is possible that the relief across the study area influenced the spatial structure of the temperature measurements. The mesa below the flight path is oriented primarily in a north-south direction. Wind shear, generated through frictional drag caused by the abrupt change in surface elevation, likely contributed at least partially to the spatial discontinuity in the temperature measurements in the north-south direction. Additional research is needed to determine the exact nature of these terrain impacts.

5 Conclusion

This study used variogram analysis to model the structure and anisotropy of temperature measurements collected from a sUAS in an ABL. We found that temperature measurements in the direction of the measured mean wind direction were less spatially continuous than those captured transverse of the mean wind direction. This structure is likely due to a combination of mechanical mixing in the ABL and the forces of wind shear caused by the topography of the study area. Additionally, the spatial structure depicted in the directional variogram most closely aligned with the mean wind direction, which corresponded to the expected ABL turbulence scale of approximately 1 km, thus supporting prior theories.

Acknowledgments

This research is supported by a grant from the U.S. National Science Foundation (NSF) [IIA-1539070] "RII Track-2 FEC: Unmanned Aircraft Systems for Atmospheric Physics". The authors thank Dr. Jamey Jacob, Marc Hartman, and Jordan Feight from Oklahoma State University for assistance with mission planning and data collection.

References

- Bendix, J., Fries, A., Zárate, J., Trachte, K., Rollenbeck, R., Pucha-Cofrep, F., Paladines, R., Palacios, I., Orellana, J., Oñate-Valdivieso, F. and Naranjo, C. (2017) RadarNet-Sur first weather radar network in tropical high mountains. *Bulletin of the American Meteorological Society*, 98(6), 1235-1254.
- Cressie, N.A.C. (1993) *Statistics for spatial data*. New York, Wiley.
- Frazier, A.E., Mathews, A.J., Hemingway, B.L., Crick, C., Martin, E. and Smith, S.W., Integrating small unmanned aircraft systems (sUAS) into meteorology and atmospheric science: challenges and opportunities for GIScience. *GI_Forum 2017*, 2, 189-199.
- Frew, E.W., Elston, J., Argrow, B., Houston, A. and Rasmussen, E. (2012) Sampling severe local storms and

- related phenomena: Using unmanned aircraft systems. *IEEE Robotics & Automation Magazine*, 19(1), 85-95.
- Hemingway, B.L., Frazier, A.E., Elbing, B.R. and Jacob, J.D. (2017) Vertical sampling scales for atmospheric boundary layer measurements from small unmanned aircraft systems (sUAS). *Atmosphere*, 8(9), 176.
- Hill, M., Konrad, T., Meyer, J., Rowland, J. (1970) A small, radio-controlled aircraft as a platform for meteorological sensors. *Appl. Phys. Lab. Tech. Digest*, 10, 11–19.
- Houston, A.L., Argrow, B., Elston, J., Lahowetz, J., Frew, E.W. and Kennedy, P.C. (2012) The collaborative Colorado–Nebraska unmanned aircraft system experiment. *Bulletin of the American Meteorological Society*, 93(1), 39-54.
- Isaaks, E.H.; Srivastava, R.M. (1989) *Applied geostatistics*. New York, Oxford University Press.
- Knuth, S.L., Cassano, J.J., Maslanik, J.A., Herrmann, P.D., Kernebone, P.A., Crocker, R.I. and Logan, N.J. (2013) Unmanned aircraft system measurements of the atmospheric boundary layer over Terra Nova Bay, Antarctica. *Earth System Science Data*, 5(1), 57.
- LaDue, D.S., Heinselmann, P.L. and Newman, J.F. (2010) Strengths and limitations of current radar systems for two stakeholder groups in the southern plains. *Bulletin of the American Meteorological Society*, 91(7), 899-910.
- Mayer, S., Sandvik, A., Jonassen, M.O. and Reuder, J. (2012) Atmospheric profiling with the UAS SUMO: a new perspective for the evaluation of fine-scale atmospheric models. *Meteorology and Atmospheric Physics*, 116(1-2), 15-26.
- McPherson, R.A., Fiebrich, C.A., Crawford, K.C., Kilby, J.R., Grimsley, D.L., Martinez, J.E., Basara, J.B., Illston, B.G., Morris, D.A., Kloesel, K.A. and Melvin, A.D., (2007) Statewide monitoring of the mesoscale environment: A technical update on the Oklahoma Mesonet. *Journal of Atmospheric and Oceanic Technology*, 24(3), 301-321.
- Oliver, M.A. and Webster, R. (2015) *Basic steps in geostatistics: the variogram and kriging*. New York, Springer.
- Pebesma, E.J. (2004) Multivariable geostatistics in S: the gstat package. *Computers & Geosciences*, 30(7), 683-691.
- Stull, R.B. (1988) *An introduction to boundary layer meteorology*, Dordrecht Kluwer Academic Publishers.